In-beam γ-ray spectroscopy of excited states in ^{141}Pm

R. Aryaeinejad,* P. M. Walker,† R. B. Firestone,‡ and Wm. C. McHarris
National Superconducting Cyclotron Laboratory and Departments of Chemistry and Physics, Michigan State University, East Lansing, Michigan 48824

(Received 25 January 1985; revised manuscript received 3 September 1985)

The level structure of the $N=80$ nucleus ^{141}Pm has been studied in-beam by the ^{142}Nd(p,2nγ)^{141}Pm reaction using a 25-MeV p beam and by the ^{141}Pr(α,4nγ)^{141}Pm reaction using a 47-MeV α beam. γ-ray singles, γ-γ coincidence (both prompt and delayed), and angular distribution experiments were performed. We found 42 γ rays deexciting 28 states in ^{141}Pm from the (p,2nγ) reaction and 34 γ rays deexciting 22 (generally higher-spin) states from the (α,4nγ) reaction, for a total of 35 known states in ^{141}Pm. These in-beam experiments, taken together with the results from ^{141}Sm^{m+g} decay, yield J^{π} assignments for most of the states and have allowed us to deduce the configurations for many of the states. The structures are discussed in terms of single-quasiparticle shell-model and triaxial weak-coupled collective states and are compared with systematics for this nuclear region.

I. INTRODUCTION

This paper concerns one of our studies of states in the odd-mass $N=80$ isotones, $^{143}_{63}$Eu$_{80}$, $^{141}_{61}$Pm$_{80}$, and $^{139}_{59}$Pr$_{80}$. A previous paper reported our results on the states in ^{143}Eu.[1] These three nuclei comprise an interesting region for study because they are transitional nuclei, amenable to interpretation both by the simple (spherical) shell model and also by various collective and deformed models. As a series they serve as a particularly valuable test of the various models (cf. Ref. 1).

The initial investigations of low-lying states in ^{141}Pm were by the β decay of ^{141}Sm^{m} (Ref. 2) and ^{141}Sm^{g} (Ref. 3). These studies included measurements of the parent half-lives, γ-ray spectra, γ-γ coincidences, the internal-conversion e$^-$ spectrum, and the half-life of the 628.6-keV metastable state. They provided much valuable information, but only selected states below 3 MeV could be populated, and unambiguous J^{π} assignments could not be made for many of these. More extensive data were obtained by Piiparinen *et al.*,[4] who performed the first in-beam γ-ray studies on states in ^{141}Pm. Using p-, ^{3}He-, and α-induced reactions, they observed 17 new states with spins up to $\frac{19}{2}^-$, states that could not have been seen via β^+/ϵ-decay studies.

In this paper we report improved in-beam γ-ray results. We have used both the ^{142}Nd(p,2nγ)^{141}Pm and the ^{141}Pr(α,4nγ)^{141}Pm reactions in order to obtain contrasting data about low-spin and somewhat higher-spin states. For each reaction we used a combination of γ-ray singles, γ-γ coincidence (both prompt and delayed), and angular-distribution experiments. We observed more γ rays than the previous investigators, and with our data we were able to resolve a number of discrepancies found in both the decay scheme and the previous in-beam γ-ray experiments.

With the results from the ^{142}Nd(p,2nγ)^{141}Pm reaction we were able to construct a level scheme containing 28 excited states in ^{141}Pm depopulated by 42 γ transitions. With results from the ^{141}Pr(α,4nγ)^{141}Pm reaction we were able to construct a similar scheme containing 22 excited states depopulated by 34 γ transitions. We analyze and discuss these states in terms of the spherical shell model and also the triaxial weak-coupling model of Meyer-ter-Vehn.[5]

II. THE ^{142}Nd(p,2nγ)^{141}Pm REACTION

A. Target and reaction

The targets were prepared by drying a thin slurry of 99.9% enriched ^{142}Nd$_2$O$_3$ (obtained from Oak Ridge National Laboratory) on a thin (0.0025-cm thick) Formvar backing. Targets were typically a few mg/cm^2 thick.

The targets were bombarded with a 25-MeV p beam from the Michigan State University 50-MeV sector-focused cyclotron to maximize the ^{142}Nd(p,2nγ)^{141}Pm reaction. Excitation functions were calculated by the compound-nucleus evaporation code CS8N,[6] and both these and the experiments showed that the only major contaminant produced in-beam was ^{142}Pm. The half-lives of ^{141}Pm and ^{142}Pm are 20.9 min (Ref. 2) and 40.5 sec,[7] respectively. Their β^+/ϵ decays also contributed to the γ-ray spectra, but these γ rays could be easily identified.

B. γ-ray singles spectra

The ^{142}Nd(p,2nγ)^{141}Pm singles γ-ray spectra were obtained with a 17%-efficient true coaxial Ge(Li) detector having a resolution of 1.9 keV FWHM. They were normally taken at 125° from the beam direction (to minimize angular distribution effects, 125° being a zero of P_2). The usual beam current was $\approx$1 nA, with the detector 20 cm from the target, resulting in a count rate of 6000—8000 counts/sec. A Cu-Cd absorber was used to shield the detector from x rays which would otherwise dominate the spectrum. A γ-ray singles spectrum taken over a 2.5-h period is shown in Fig. 1.

A total of 42 γ rays were assigned to ^{141}Pm from the

TABLE I. γ transitions observed in the ^{142}Nd(p,2nγ)^{141}Pm reaction.

E_γ (keV)	I_γ	Angular distribution coefficients A_2/A_0	A_4/A_0	Multipolarity Conversion[a]	Angular distribution
196.6±0.1[b]	186 ±11[c]	−0.02±0.01	−0.02±0.01	*M*1	
197.3±0.2[b]	?				
208.7±0.1[b]	weak				
247.4±0.2	1.5±0.2	−0.25±0.12	−0.03±0.19		dipole
324.6±0.1[b]	6.8±0.5	−0.08±0.02	0.05±0.03	*M*1	dipole
402.6±0.2	?				
403.8±0.1[b]	31 ±2	−0.10±0.02	0.04±0.02	*M*1 + *E*2	
431.8±0.1[b]	≡100	isotropic	isotropic	*M*2	
438.8±0.1	12.7±1.2	−0.28±0.22	0.25±0.25	*E*2	dipole
524.9±0.2	weak				
531.3±0.2	3.2±0.3	0.15±0.08	0.19±0.11		quadrupole
538.5±0.2	18.9±1.2	−0.34±0.02	0.02±0.02	*M*1	dipole
607.9±0.2	3.6±0.5	−0.06±0.06	−0.06±0.10		
628.6±0.1[b]	7.1±0.5	0.01±0.02	0.01±0.04	*E*3[d]	
640.5±0.2	weak				
653.9±0.2[b]	1.2±0.1				
684.7±0.2[b]	29 ±2	−0.77±0.01	0.06±0.02	*M*1 + *E*2	dipole
694.0±0.2	8.4±0.8	−0.11±0.04	0.09±0.06		dipole
702.1±0.1[b]	5.4±0.6	−0.90±0.03	−0.15±0.06		dipole
728.3±0.1[b,e]	12.8±0.8	−0.5 ±0.03	−0.60±0.11		dipole
749.6±0.1	3.4±0.4				
777.6±0.1	36 ±2	0.27±0.01	−0.05±0.01	*E*2	quadrupole
785.3±0.2[e]	10.6±0.8	−0.34±0.04	0.04±0.06	*E*2	dipole?
820.6±0.2	1.9±0.6				
827.9±0.3	1.4±0.5				
837.1±0.1[b]	30 ±2	0.20±0.03	−0.06±0.04		quadrupole
858.5±0.3	14.1±0.8	0.26±0.01	−0.02±0.01		quadrupole
882.0±0.1[b]	30 ±2	0.26±0.02	−0.11±0.04		quadrupole
911.4±0.2[b]	16.1±1.0	0.04±0.02	0.12±0.02	*E*2	?
924.7±0.3	weak				
956.5±0.3	9.8±0.7	−0.30±0.07	−0.30±0.12		dipole
995.7±0.2[b]	6.6±0.5	0.44±0.06	0.06±0.09		quadrupole
1008.7±0.3	5.0±0.4	−0.43±0.04	−0.10±0.06		dipole
1037.5±0.3	4.1±0.3	0.35±0.09	−0.03±0.16		quadrupole
1045.9±0.4	3.5±0.3	0.14±0.01	−0.13±0.02		quadrupole
1153.3±0.3	1.0±0.2	−0.49±0.05	−0.14±0.11		dipole
1163.0±0.3[b]	3.4±0.3	0.29±0.03	−0.11±0.06		quadrupole
1242.5±0.4	1.7±0.2	−0.15±0.06	−0.05±0.09		dipole
1495.9±0.4	1.9±0.2				
1786.3±0.4	0.6±0.2				

[a]Transition multipolarities determined with the aid of conversion electrons given in Ref. 4.
[b]These transitions were seen in both the (p,2nγ) and the (α,4nγ) reactions; therefore, the quoted energies are a weighted average of the values obtained from the two reactions.
[c]Part of this intensity belongs to the 197.3-keV transition.
[d]Assigned *E*3 on the basis of its half-life.
[e]Doublet.

(p,2nγ) reaction on the basis of these γ-ray singles spectra and the γ-γ coincidence experiments discussed in Sec. II C. The γ rays are listed in Table I, together with their relative intensities. All of the data analysis was performed using the computer code SAMPO.[8] Energy calibrations were performed by counting simultaneously with ^{60}Co, ^{152}Eu, and ^{226}Ra standards and cross comparing with some of the ^{141}Pm γ rays already characterized from ^{141}Sm decay.[2,3] The errors quoted for the energies include estimated errors in the standards and are based primarily on the reproducibility of a peak and its height above background. The intensities were derived from an extensive set of experimental detector efficiency curves; errors on the intensities are based primarily on the statistical reproducibility of a given peak. The relative intensities of those transitions that were components of unresolvable doublets are indicated by question marks.

Piiparinen *et al.*[4] studied the ^{142}Nd(p,2nγ)^{141}Pm reac-

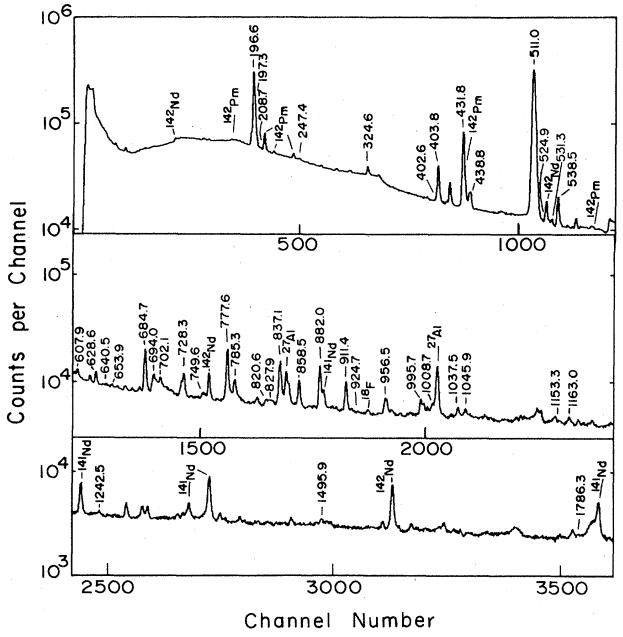

FIG. 1. In-beam singles γ-ray spectrum from the reaction ^{142}Nd(p,2nγ)^{141}Pm using a 25-MeV p beam.

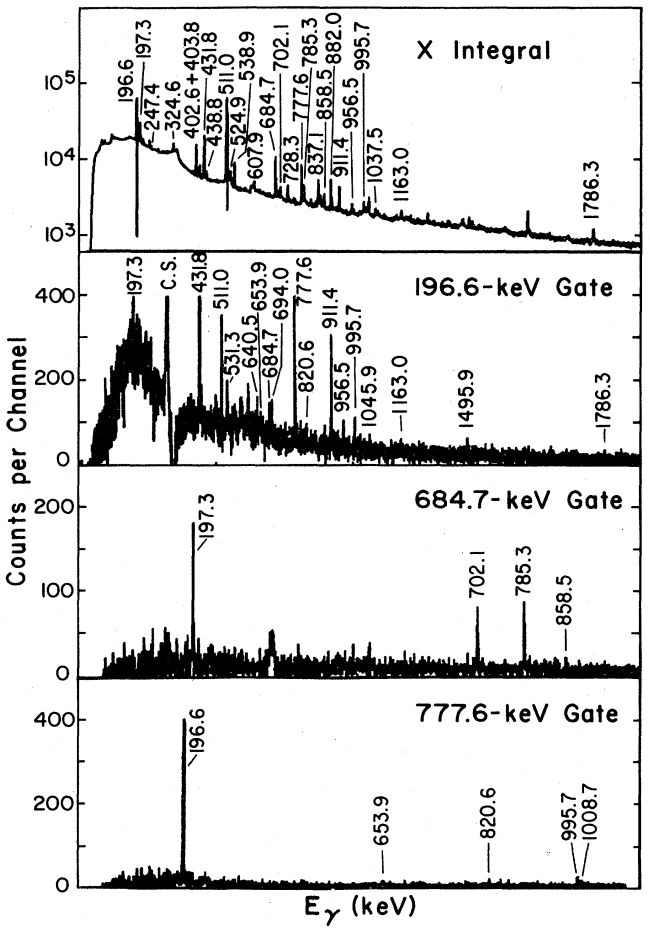

FIG. 2. In-beam γ-γ coincidence spectra from the reaction ^{142}Nd(p,2nγ)^{141}Pm. The integrated coincidence spectrum ("all events") is shown at the top, with three representative gated spectra below it.

tion but at somewhat lower energies, stopping with $E_p = 20$ MeV. They list 32 γ rays from this reaction. We agree reasonably well with their results for the more intense transitions, but they did not observe 15 of our weaker transitions (although they did observe three of these in α- and ^{3}He-induced reactions), and we did not observe seven of their weaker transitions. (They observed a number of these lines in both p- and ^{3}He-induced reactions but not in the α-induced reactions, which were performed at another laboratory—this leads one to suspect the possibility of background or contaminants.)

C. γ-γ coincidence spectra

The 25-MeV p beam was also used for γ-γ coincidence experiments. For these, two true-coaxial Ge(Li) detectors were used; one was 10% efficient (energy resolution 2.4 keV FWHM), the other 16% efficient (2.6-keV FWHM). A standard three-parameter ($E_\gamma \times E_\gamma \times t$) fast-slow coincidence setup with constant-fraction timing was used. In these "megachannel" experiments the coincidences were recorded event by event on magnetic tape for later off-line sorting with background subtraction. A resolving time of ≈ 100 nsec (2τ) was used. Approximately 7×10^7 events were recorded.

Representative coincidence spectra are shown in Fig. 2. The integral coincidence spectrum (all coincident events as recorded by the 10% detector) is at the top, and three important gated spectra are shown below it. A summary of the coincidence results is given in Table II.

D. γ-ray angular distributions

Again, for the γ-ray angular distribution experiments the p-beam energy was 25 MeV. The same 17%-efficient Ge(Li) detector was used as was used for obtaining the γ-ray singles spectra. Spectra were taken at 90°, 100°, 110°, 125°, 140°, and 155° with respect to the beam direction. The angles were selected in random order for the various experiments, and data were typically collected for 2.5 h at each angle.

The isotropic 431.8-keV transition was used as an internal normalization for the spectra taken at different angles. Peak intensities were derived from the peak-fitting program SAMPO. After the normalization of the γ-ray peak areas, least-squares fits to the experimental angular distributions were made, using the computer code GADFIT.[9] The fits were made to the usual equation,

$$I = 1 + (A_2/A_0)P_2(\cos\theta) + (A_4/A_0)P_4(\cos\theta) .$$

The parameters extracted from the fit, A_2/A_0 and A_4/A_0, are included in Table I. The A_2 and A_4 values for the 196.6- and 628.6-keV transitions turned out to be close to zero, as expected, because of the relatively long half-life of the 628.4-keV metastable state. Values of

TABLE II. Summary of coincidence results for the ^{142}Nd(p,2nγ)^{141}Pm reaction.

Gated γ ray (keV)	Coincident γ rays (keV)
196.6	197.3,431.8,531.3,607.9, 640.5,653.9,684,7,694.0, 777.6,820.6,911.4,956.5, 995.7,1045.9,1163.0,1495.9, 1786.3
208.7	196.6,431.8,1037.5
247.4	538.5
324.6	403.7
402.6+403.8	196.6,324.6,728.3,749.6, 911.4
431.8	196.6,208.7
438.8	
531.3	196.6
538.5	247.4,924.7
607.9	196.6
628.6	
640.5	196.6,1037.5
653.9	196.6,777.6
684.7	197.3,702.1,785.3,858.5
694.0	196.6,911.4
702.1	684.7
728.3[a]	402.6,882.0
749.6	403.8
777.6	196.6,653.9,820.6,995.7, 1008.7
785.3[a]	684.7
820.6	196.6,777.6
827.9	196.6,777.6
837.1	1037.5
858.5	684.7
882.0	728.3
911.4	196.6,402.6,694.0
924.7	538.5
956.5	196.6
995.7	196.6,777.6
1008.7	196.6,777.6
1037.5	196.6,208.7,640.5,837.1
1045.9	196.6
1163.0	196.6
1495.9	196.6
1786.3	196.6

[a]Doublet.

A_2/A_0 were, in general, more reliable than the values of A_4/A_0 and could be used to estimate the mixing ratios for the more intense transitions. Some representative angular distributions, together with their calculated fits, are shown in Fig. 3.

III. THE ^{141}Pr(α,4nγ)^{141}Pm REACTION

A. Target and reaction

The ^{141}Pr(α,4nγ)^{141}Pm reaction was used for preferential population of the higher-spin states in ^{141}Pm. Targets were prepared in a similar fashion to that used for the p-induced reaction, except that a slurry of 99.99%-pure

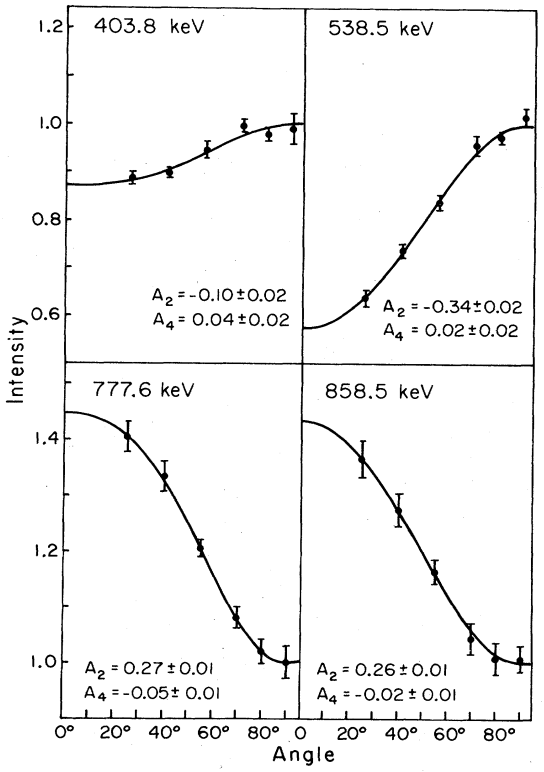

FIG. 3. Four representative angular distributions of γ rays from the reaction ^{142}Nd(p,2nγ)^{141}Pm together with their fits calculated by the code GADFIT. The points correspond to 90° and the backward angles, 100°, 110°, 125°, 140°, and 155°.

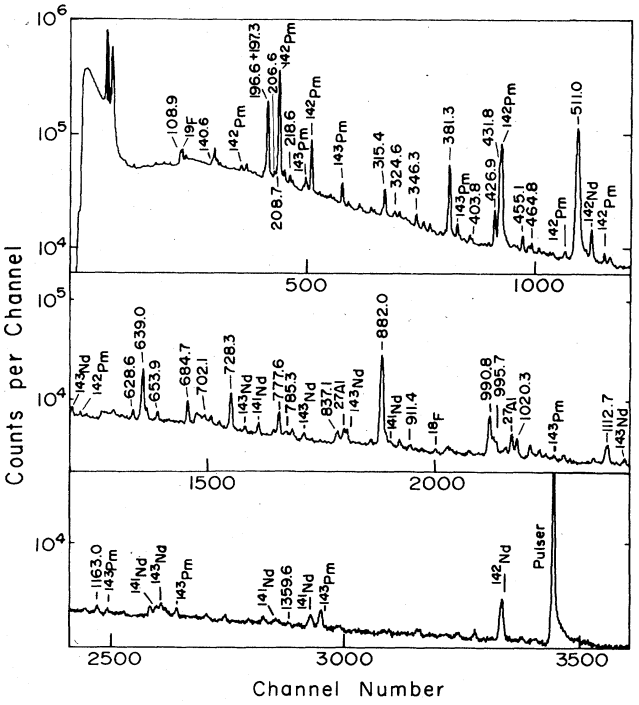

FIG. 4. In-beam singles γ-ray spectrum from the reaction ^{141}Pr(α,4nγ)^{141}Pm using a 47-MeV α beam.

natural Pr_2O_3 was used.

Excitation functions calculated by the code CS8N (Ref. 6) indicate that the optimum α energy for the (α,4n) reaction to minimize contaminant γ rays from other reactions would be 54 MeV. At this energy the contaminants from the (α,3n) and (α,5n) reactions are only about 4% of the total. However, the highest routinely available α beam from our cyclotron was 47 MeV, and this is what we used for all of our experiments. At 47 MeV the principal contaminant, ^{142}Pm, is about 34% of the total. Other in-beam contaminants produced to a lesser extent are ^{143}Pm and ^{143}Nd. Also, the β^+/ϵ decays of ^{141}Pm and ^{142}Pm contributed to the γ-ray spectra, as did products resulting from oxygen in the targets.

B. γ-ray singles spectra

We used a 7.7% efficient true coaxial Ge(Li) detector having a resolution of 1.9 keV FWHM to obtain the singles γ-ray spectra for the ^{141}Pr(α,4nγ)^{141}Pm reaction. Other than this and the need for a 10-nA 47-MeV α beam, the experiments were conducted in an identical manner to that described in Sec. II B for the ^{142}Nd(p,2nγ)^{141}Pm γ-ray singles spectra. A singles γ-ray spectrum taken over a 2.5-h period is shown in Fig. 4.

A total of 35 γ rays were assigned to ^{141}Pm from the (α,4nγ) reaction on the basis of γ-ray singles and γ-γ coincidence spectra. These are listed in Table III, together with their relative intensities. The intensities of those

TABLE III. γ transitions observed in the ^{141}Pr(α,4nγ)^{141}Pm reaction.

		Angular distribution coefficients		Multipolarity	
E_γ (keV)	I_γ	A_2/A_0	A_4/A_0	Conversion[a]	Angular distribution
108.9±0.2	?				
140.6±0.2	10.3±1.2	−0.13±0.07	−0.03±0.10		dipole
196.6±0.1[b]	138 ±9[c]	−0.06±0.06	−0.02±0.07	$M1$	dipole
197.3±0.2[b]	?				
206.6±0.2	weak				
208.7±0.1[b]	?				
218.6±0.2	3.1±0.2				
315.4±0.1	34 ±1	−0.18±0.05	0.02±0.07		dipole
324.6±0.1[b]	5.7±0.1	−0.26±0.07	0.02±0.09	$M1$	dipole
346.3±0.2	10.9±0.4	−0.44±0.03	−0.01±0.04		dipole
381.3±0.1	107 ±3[d]	−0.11±0.03	0.02±0.05		dipole
403.8±0.1	2.7±0.4			$M1 + E2$	
426.9±0.1	21 ±1	−0.39±0.04	0.03±0.05		dipole
431.8±0.1[b]	≡100	0.02±0.02	0.04±0.04	$M2$	
455.1±0.2	7.8±0.7	0.30±0.06	0.04±0.08		quadrupole
464.8±0.2	5.1±0.5	−0.22±0.05	0.12±0.07		dipole
628.6±0.1[b]	6.1±0.4	0.07±0.03	0.04±0.04	$E3$[e]	
639.0±0.1	44 ±1	−0.02±0.03	0.02±0.04		
653.9±0.2[b]	4.2±0.5	−0.50±0.07	0.08±0.10		dipole
684.7±0.2[b]	11.2±0.4	−0.89±0.02	0.08±0.03	$M1 + E2$	dipole
702.1±0.1[b]	3.5±0.3	−0.59±0.02	0.01±0.03		dipole
723.3±0.2[f]	22.3±0.5	0.28±0.03	−0.02±0.05		quadrupole
777.6±0.1[b]	10.3±0.2	0.32±0.04	0.01±0.06	$E2$	quadrupole
785.3±0.2[f]	1.3±0.2	−0.93±0.09	0.27±0.12	$E2$	dipole?
837.1±0.1[b]	3.1±0.2	0.22±0.08	−0.06±0.12		quadrupole
882.0±0.1[b]	85 ±2	0.06±0.02	−0.02±0.04		quadrupole
911.4±0.2[b]	1.4±0.2			$E2$	
990.8±0.2	16.0±0.4	−0.22±0.02	0.02±0.03		dipole
995.7±0.2[b]	4.8±0.2	0.41±0.03	0.03±0.04		quadrupole
1020.3±0.3	5.1±0.2	−0.03±0.03	−0.04±0.04		
1112.7±0.2	4.1±0.2	−0.15±0.04	0.18±0.05		dipole
1163.0±0.3[b]	1.5±0.1	0.15±0.06	0.02±0.09		quadrupole
1359.6±0.4	weak				

[a]Transition multipolarities determined with the aid of conversion electrons given in Ref. 4.
[b]These transitions were seen in both the (α,4nγ) and the (p,2nγ) reactions; therefore, the quoted energies are a weighted average of the values obtained from the two reactions.
[c]Part of this intensity belongs to the 197.3-keV transition.
[d]Possibly some contribution from ^{140}Pm.
[e]Assigned $E3$ on the basis of its half-life.
[f]Doublet.

transitions that were components of unresolvable doublets are indicated by question marks. In general, γ rays are not listed in this table unless they were placed on the basis of coincidence data.

We find the same sort of inconsistencies here with the data of Piiparinen *et al.*[4] as we did with the ^{142}Nd(p,2nγ)^{141}Pm reaction (cf. Sec. II B). They list 24 transitions from this reaction, and we overlap on only 14 of them. Two of our α-induced transitions were reserved in their p- and/or ^{3}He-induced reactions but not in their α-induced reactions.

C. γ-γ coincidence spectra

The 7.7%- and 16%-efficient Ge(Li) detectors were used for the γ-γ coincidence experiments, using the same procedures described in Sec. II C for the p-induced reaction. Using a resolving time of $\approx$100 nsec, 1.5×10^7 events were recorded on magnetic tape for analysis.

Representative coincidence spectra are shown in Fig. 5, with the integral coincidence spectrum (7.7% detector) at the top and five important gated spectra below. A summary of the coincidence results is given in Table IV.

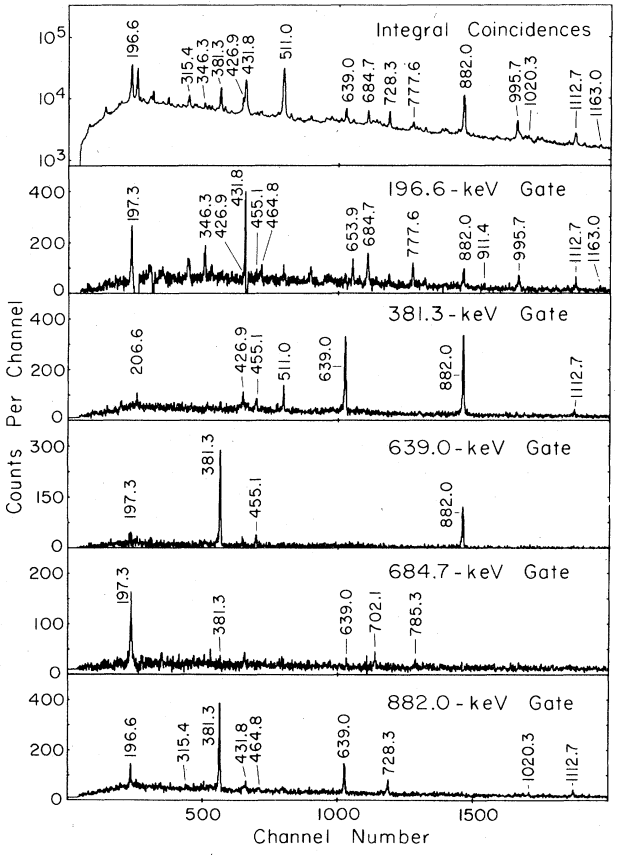

FIG. 5. In-beam γ-γ coincidence spectra from the reaction ^{141}Pr(α,4nγ)^{141}Pm. The integral coincidence spectrum is shown at the top, with five representative gated spectra below it.

TABLE IV. Summary of coincidence results for the ^{141}Pr(α,4nγ)^{141}Pm reaction.

Gated γ ray (keV)	Coincident γ rays (keV)
108.9	324.6,403.8,728.3
196.6	197.3,346.3,426.9,431.8, 455.1,464.8,653.9,684.7, 777.6,882.0,911.4,995.7, 1112.7,1163.0
208.7	196.6,431.8,728.3
315.4	728.3,882.0
324.6	108.9,403.8
346.3	197.3,381.3,882.0
381.3	206.6,426.9,455.1,639.0, 882.0,1112.7
403.8	108.9,324.6,728.3
426.9	206.6,381.3,455.1,639.0 1020.3,1112.7
431.8	196.6,346.3,381.3,426.9 684.7,882.0
455.1	381.1,426.9,639.0,728.3
464.8	197.3,728.3,882.0
628.6	
639.0	197.3,381.3,455.1,882.0
653.9	196.6,777.6
684.7	197.3,381.3,639.0,702.1, 785.3
702.1	684.7
728.3[a]	108.9,197.3,315.4,464.8, 882.0
777.6	196.6,653.9,995.7
785.3[a]	684.7
882.0	196.6,315.4,381.3,431.8, 464.8,639.0,728.3,1020.3, 1112.7
911.4	196.6,990.8
990.8	196.6,911.4
1020.3	882.0
1112.7	197.3,381.3,882.0
1163.0	196.6

[a]Doublet

D. γ-ray angular distributions

Using the 7.7%-efficient Ge(Li) detector, the γ-ray angular distributions were obtained in a fashion similar to that described in Sec. II D for the p-induced reaction. The normalization was provided by using the 16%-efficient Ge(Li) detector in a stationary position at 45°. The A_2/A_0 and A_4/A_0 values obtained are included in Table III. The A_2 and A_4 values for the 196.6-, 431.8-, and 628.6-keV transitions were found to be close to zero, as expected from the relatively long half-life of the 628.6-keV metastable state. Angular distribution coefficients not listed in the table belong to γ rays that are either part of unresolvable multiplets or too weak for accurate peak fitting. Some representative angular distributions, together with their calculated fits, are shown in Fig. 6.

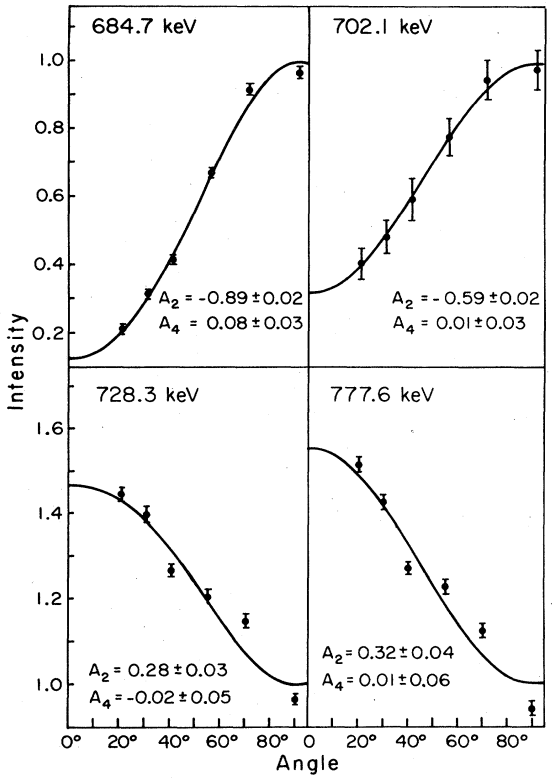

FIG. 6. Four repesentative angular distributions of γ rays from the reaction ^{141}Pr(α,4nγ)^{141}Pm together with their fits calculated by GADFIT.

IV. THE ^{141}Pm LEVEL SCHEME

Since the ^{141}Pr(α,4nγ)^{141}Pm reaction tends to populate high-spin states and the ^{142}Nd(p,2nγ)^{141}Pm reaction tends to populate somewhat lower-spin states, we have constructed separate ^{141}Pm level schemes for the two reactions. Coincidence data, intensity balances, and conversion coefficients [plus delayed-coincidence spectra in the case of the (α,4nγ) reaction] were the primary factors used to construct the level schemes. Secondary factors were energy summing relationships, input from the known ^{141}Sm^{m} (Ref. 2) and ^{141}Sm^{g} (Ref. 3) decay schemes, and our angular distribution data. The J^{π} assignments were made on the basis of angular distribution coefficients, conversion coefficients, an input from the ^{141}Sm^{m+g} decay schemes. The ^{141}Pm level scheme deduced from the (p,2nγ) reaction is shown in Fig. 7; that from the (α,4nγ) reaction, in Fig. 8.

This section is broken into three parts: (A), construction of the ^{141}Pm level scheme from the (p,2nγ) reaction, (B) construction of the ^{141}Pm level scheme from the (α,4nγ) reaction, and (C) comparison of the results obtained from the two reactions and from other experiments.

A. ^{141}Pm level scheme from the ^{142}Nd(p,2nγ)^{141}Pm reaction

Ground, 196.6-, and 628.4-keV states

The J^{π} of the ground state is known[2,10,11] to be $\frac{5}{2}^{+}$, and the well-known 196.6- and 628.4-keV states have been

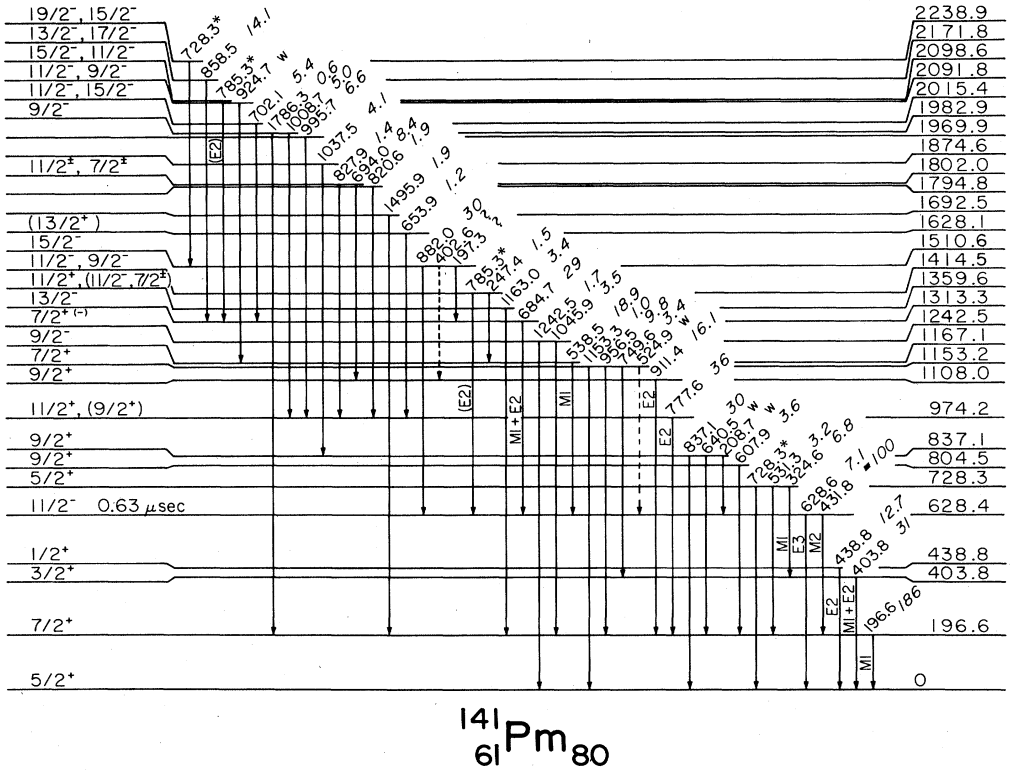

FIG. 7. ^{141}Pm level scheme as determined from the ^{142}Nd(p,2nγ)^{141}Pm reaction.

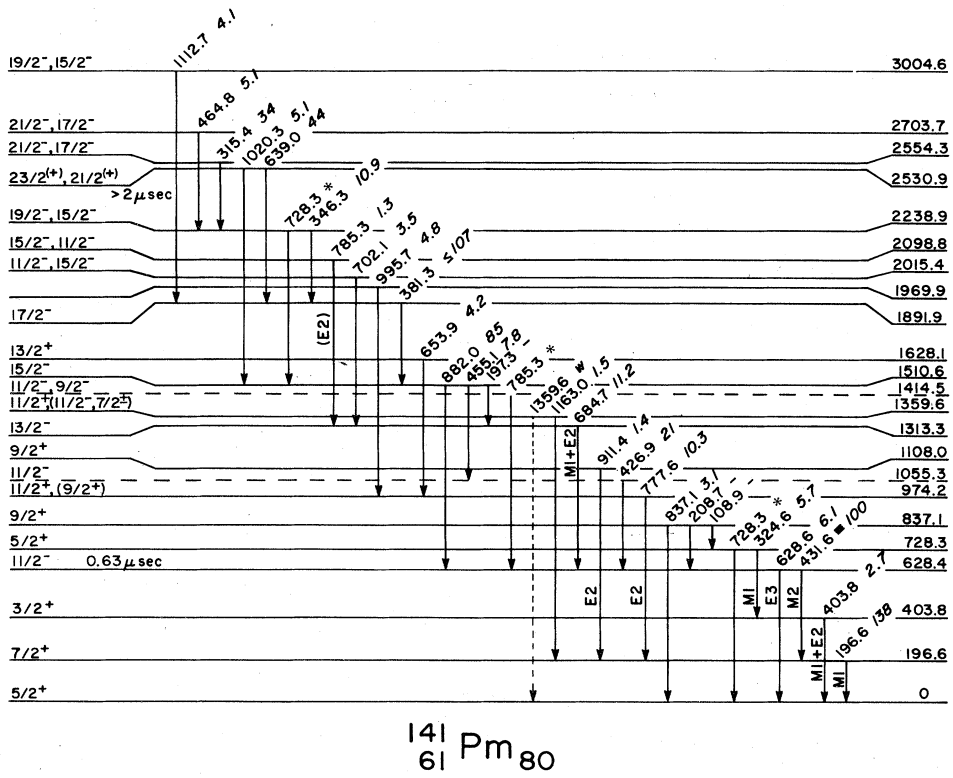

$^{141}_{61}Pm_{80}$

FIG. 8. ^{141}Pm level scheme as determined from the ^{141}Pr$(\alpha,4n\gamma)^{141}$Pm reaction. [During a final check in the internal consistency of this level scheme, using the program SPIN developed at Lawrence Berkeley Laboratory by one of the authors (R.B.F.), we could also place the additional γ transitions: 108.9 (837.1→728.3), 140.6 (2238.9→2098.8), and 206.6 keV (2098.8→1891.9).]

assigned $\frac{7}{2}^+$ and $\frac{11}{2}^-$, respectively, on the basis of the multipolarities of the 196.6- , 431.8-, and 628.6-keV transitions, together with the logft values from ^{141}Sm^m decay. The half-life of the 628.4-keV state has been measured to be 0.70±0.02 μsec (Ref. 12) and 0.59±0.02 μsec.[3] (We exclude an earlier measurement[13] of 0.22±0.01 μsec.) Because of this discrepancy, we remeasured its half-life, using the $(\alpha,4n\gamma)$ reaction (cf. Sec. IV B) and obtained a value of 0.63±0.02 μsec.

Because of the 628.4-keV state is metastable, one expects the 431.8- and 628.6-keV transitions to be isotropic. Also, because the 628.4-keV state contributes a large portion of the feeding to the 196.6-keV state and because the remainder of the feeding to the latter state is rather complex in nature, one expects the 196.6-keV transition to approach being isotropic. These expectations were borne out from both the (p,2nγ) and the $(\alpha,4n\gamma)$ reactions. Although this information does not permit us to comment further on the J^π assignments, it adds to the consistency of the previous arguments.

No particle-transfer reactions have yet been used to populate states in ^{141}Pm. However, such reactions[14] have established that in the corresponding odd-mass $N=82$ nuclei the low-lying $g_{7/2}$, $d_{5/2}$, and $h_{11/2}$ states, in particular, are excellent single-particle states. We do not anticipate their being quite so pure in $N=80$ nuclei such as ^{141}Pm; nevertheless, the ground, 196.6-, and 628.4-keV states should consist primarily of the $\pi d_{5/2}$, $\pi g_{7/2}^{-1}$, and $\pi h_{11/2}$ single-particle states.

403.8-, 438.8-, and 728.3-keV states

The fact that the 438.8-keV γ ray was not found to be in coincidence with any other leads to the placement of the 438.8-keV state. It was assigned $\frac{1}{2}^+$ on the basis[3] of direct β^+/ϵ feeding from ^{141}Sm^g and by additional γ-ray feeding from the six higher-lying, low-spin states. We would not expect to have seen appreciable population of these low-spin states at higher excitations via our (p,2nγ) reaction; thus, the large errors in our angular distribution coefficients prevent them from contributing to a J^π assignment. However, our data are consistent with $\frac{1}{2}^+$.

From the 403.8-keV gated spectrum (which includes the 402.6-keV gate), there is evidence for coincidences with the 324.6- and 749.6-keV γ rays. (The other γ rays listed in this entry in Table II are in coincidence with the 402.6-keV γ ray.) Intensity balances suggest states at 403.8, 728.3, and 1153.2 keV.

The 403.8-keV transition is mixed $M1+E2$, restricting J^π to $\frac{3}{2}^+$, $\frac{5}{2}^+$, or $\frac{7}{2}^+$. The $\frac{5}{2}^+$ value is ruled out because of the large negative A_2 and small positive A_4. The ^{141}Sm^g β^+/ϵ-decay logft value of 5.8 rules out $\frac{7}{2}^+$. Thus, the 403.8-keV state is undoubtedly $\frac{3}{2}^+$.

The 728.3-keV state feeds into the $\frac{5}{2}^+$ ground, the $\frac{7}{2}^+$ 196.6-, and the $\frac{3}{2}^+$ 403.8-keV states by the 728.3-, 531.3-, and 324.6-keV γ rays. From ^{141}Sm^g decay an $M1$ or $E2$ multipolarity was assigned to the 324.6-keV transition. Our data are consistent with an almost pure $M1$, which

limits J^π to $\frac{1}{2}^+$, $\frac{3}{2}^+$, or $\frac{5}{2}^+$. The $\frac{3}{2}^+$ value is eliminated because of the negative A_2 and small positive A_4. Also, the absence of a measurable half-life rules out the possibility of $M3$ for the 531.3-keV transition, eliminating $\frac{1}{2}^+$ as well. (The nonisotropic angular distributions also rule out $\frac{1}{2}$.) All of this (including the ^{141}Sm^g logft value of 6.8) leads to a $\frac{5}{2}^+$ assignment.

The major components of the wave functions of the 403.8- and 438.8-keV states should be the $\pi d_{3/2}$ and $\pi s_{1/2}$ single-particle states, although these (the $\pi d_{3/2}$ state, in particular) are not expected to be nearly so pure as the other three single-proton states. The $\frac{5}{2}^+$ 728.3-keV state is more complex in nature.

837.1-keV state

This state, tentatively identified from ^{141}Sm^m decay, was placed from coincidences involving the 208.7- and 640.5-keV γ rays, the placement then corroborated by independent sum relations. The A_2 and A_4 values for the 837.1-keV ground-state transition limit J^π to $\frac{1}{2}^+$ or $\frac{9}{2}^+$. We can eliminate $\frac{1}{2}^+$ on the basis of the state being excited so strongly at this excitation by the (p,2nγ) reaction and from its γ-deexcitation pattern, leaving a definite $\frac{9}{2}^+$ assignment.

974.2-keV state

The coincidence relationship between the 777.6-keV γ ray [second most intense in the spectra from the (p,2nγ) reaction] and the 196.6-keV γ ray places this state. The multipolarity of the 777.6-keV transition is probably $E2$ (with a possibility of $E1$). Its A_2 and A_4 values are consistent with a stretched $E2$, which limits the J^π for the 974.2-keV state to $\frac{3}{2}^+$ or $\frac{11}{2}^+$. From its population by ^{141}Sm^m decay, the $\frac{3}{2}^+$ assignment can be eliminated, leaving $\frac{11}{2}^+$.

A tentative $\frac{9}{2}^+$ assignment was made for this state in Ref. 2, based primarily on the transition to the $\frac{5}{2}^+$ ground state, which would of necessity be an $M3$ with the $\frac{11}{2}^+$ assignment. The single-particle estimate for the half-life of such an $M3$ transition is 1.03×10^{-4} sec, and inasmuch as the 974.0-keV transition is a 1% branch, this implies a half-life for the 974.2-keV state in the vicinity of 1 μsec, inconsistent with what was observed. On the other hand, the negative A_4 value for the 777.6-keV γ ray rules out a mixed $M1+E2$ multipolarity, which would be expected with a $\frac{9}{2}^+$ assignment (unless the major component of the 974.2-keV state were $[\pi g_{7/2}^{-1}\times2^+]_{9/2^+}$, in which a collective $E2$ could predominate). Thus, we are left with a preference for $\frac{11}{2}^+$ but cannot rule out $\frac{9}{2}^+$.

1108.0-keV state

The coincidence relationship between the 911.4- and 196.6-keV γ rays establishes this state, which was also observed in ^{141}Sm^m decay (with no definite J^π assignment possible from that work). The small positive A_2 and large negative A_4 for the 911.4-keV γ ray are consistent with a $J+1\rightarrow J$ pure $E2$ transition, which restricts J^π to $\frac{5}{2}^+$ or $\frac{9}{2}^+$. The $\frac{5}{2}^+$ value can be ruled out, both from ^{141}Sm^m decay and because the (p,2nγ) reaction is not likely to populate so strongly the relatively low spin of $\frac{5}{2}$ at this excitation energy, leaving $J^\pi=\frac{9}{2}^+$ for this state.

1153.2-keV state

This state was placed on the basis of coincidence relationships and energy sums among the 524.9-, 749.6-, 956.5-, and 1153.3-keV γ rays, none of which has been seen from ^{141}Sm^{m+g} decays. These deexcitations restrict J^π for this state to $\frac{7}{2}^+$, which is also consistent with the angular distribution coefficients for the 956.5- and 1153.3-keV γ rays.

1167.1-keV state

This state feeds into the $\frac{11}{2}^-$ 628.4-keV state via the 538.5-keV transition. Although the long half-life of the 628.4-keV state made this impossible to confirm by a direct coincidence measurement, the other coincidence relationships with the 538.5-keV γ ray confirm the placement, as did the extensive coincidence data from ^{141}Sm^m decay. If the 538.5-keV transition is an $M1$, as it appears to be, J^π for the 1167.1-keV state is restricted to $\frac{9}{2}^-$, $\frac{11}{2}^-$, or $\frac{13}{2}^-$. The $\frac{11}{2}^-$ value is ruled out by the large negative A_2 and small positive A_4. The fact that this state is not fed by γ rays from high-spin states probably indicates it is not in the yrast sequence, eliminating $\frac{13}{2}^+$. (We show later on that the 1313.3-keV state is the yrast $\frac{13}{2}^-$ state and receives feeding from the high-spin states.) In addition, this state was not observed in the (α,4nγ) reaction. We are left with $\frac{9}{2}^-$ for this state.

1242.5-keV state

The coincident 1045.9- and 196.6-keV γ rays plus the 1242.5-keV crossover transition place the 1242.5-keV state, which was not seen in ^{141}Sm^{m+g} decays. Its J^π value is restricted to $\frac{3}{2}^\pm$, $\frac{7}{2}^\pm$, or $\frac{11}{2}^\pm$ because of the angular distributions of the 1045.9- and 1242.5-keV γ rays, whose multipolarities have not been determined. The $\frac{3}{2}^\pm$ value can be ruled out on the basis that the (p,2nγ) reaction is not likely to populate a low-spin state at this excitation. The fact that this state was not observed in the (α,4nγ) reaction (cf. below), plus the large negative A_4 for the 1045.9-keV γ ray, rule out $\frac{11}{2}^\pm$. A $\frac{7}{2}^-$ assignment would require the 1045.9- and 1242.5-keV transitions to be mixed $E1+M2$, so $\frac{7}{2}^+$ is preferable.

1313.3-keV state

Five γ rays seen in coincidence with the 684.7-keV γ ray place the 1313.3-keV state. The depopulating 684.7-keV transition appears to be $M1$ and/or $E2$, and its angular distribution coefficients are consistent with a mixed $M1+E2$. The large negative A_2 and small positive A_4 further restrict J^π to $\frac{9}{2}^-$ or $\frac{13}{2}^-$. Since this state is seen so intensely in both the (p,2nγ) and (α,4nγ) reactions and is fed so strongly by high-spin states from above, yrast arguments lead us to prefer the higher-spin assignment, $\frac{13}{2}^-$.

1359.6-keV state

We can limit the J of this previously unobserved state to $\frac{7}{2}$ or $\frac{11}{2}$ by using the angular distribution coefficients for its deexciting 1163.0-keV γ ray. The small positive A_2 and large negative A_4 give an indication of a $J+2\rightarrow J$ stretched quadrupole transition, favoring $\frac{11}{2}$. An $\frac{11}{2}^-$ assignment would require the 1163.0-keV transition to be $M2$, somewhat inconsistent with its being the sole deexciting transition. We prefer $\frac{11}{2}^+$. [A problem arises if this state deexcites to the ground state via the weak 1359.6-keV γ ray, seen in the $(\alpha,4n\gamma)$ reaction. At this point, pending better statistics and coincidence data, the most obvious way out of this difficulty is a different placement of the weak 1359.6-keV γ ray.]

1414.5-keV state

This state was seen in $^{141}Sm^m$ decay and was tentatively assigned $\frac{11}{2}^-$ or $\frac{9}{2}^-$. Our angular distribution coefficients also lead to an $\frac{11}{2}^-$ or $\frac{9}{2}^-$ assignment.

1510.6-keV state

Not observed previously, this state was populated strongly by both the (p,2nγ) and $(\alpha,4n\gamma)$ reactions. The angular distribution pattern of its deexciting 882.0-keV γ ray is consistent with a stretched $E2$, restricting J^π to $\frac{7}{2}^-$ or $\frac{15}{2}^-$. Yrast considerations lead us to prefer $\frac{15}{2}^-$.

The remaining states

Of the 12 remaining states, those at 1982.9 and 2091.8 keV had been seen previously from $^{141}Sm^m$ decay; those at 1874.6, 1969.9, 2015.4, 2098.6, and 2238.9 keV were also reported by Piiparinen *et al.*[4] Our angular distribution data are consistent with assignments of $\frac{9}{2}^-$ for the 1982.9-keV state and $\frac{11}{2}^-$ or $\frac{9}{2}^-$ for the 2091.8-keV state. In addition, we can narrow down the assignments to $\frac{11}{2}^+$ or $\frac{7}{2}^+$ for the 1802.0-keV state, to $\frac{15}{2}^-$ or $\frac{11}{2}^-$ for the 2098.0-keV state, and to $\frac{13}{2}^-$ or $\frac{17}{2}^-$ for the 2171.8-keV state. We were unable to make assignments for the remaining five states, although we would expect them to have $J \geqq \frac{7}{2}$. It is worth mentioning that our coincidence data indicate two separate 728.3-keV transitions and two separate 785.3-keV transitions.

B. ^{141}Pm level scheme from the ^{141}Pr$(\alpha,4n\gamma)^{141}$Pm reaction

Our proposed level scheme based on the ^{141}Pr$(\alpha,4n\gamma)^{141}$Pm reaction is shown in Fig. 8. The intensities are normalized to 100 for the 431.8-keV transition strength. Although this isotropic transition was selected as the best fiducial transition, it presented some difficulties: In the $(\alpha,4n\gamma)$ spectra it was part of a doublet with a 433.7-keV γ ray from ^{142}Pm; also, there is some 11% more intensity going in to the 628.4-keV state than coming out of it (even after correcting the 628.6- and 431.8-keV transitions for conversion). The placement of the 12 states that populate the 628.4-keV metastable state directly or indirectly is based on delayed coincidence spectra as well as prompt coincidence spectra, as discussed below. In the following discussion of details of constructing the level scheme and assigning J^π values, we limit ourselves to data supplemental to the (p,2nγ) reaction already discussed.

628.4-keV state

Because of the discrepancy among the measurements (see above, Sec. IV A) of the half-life of the metastable 628.4-keV state, we remeasured this value. We modified our fast-slow γ-γ coincidence system (described above in Secs. II D and III C) to include a time-to-amplitude converter (TAC) ramp of ≈ 4 μsec. The X axis (stops) was gated on the 431.8-keV region and the Y axis (starts) was gated on the entire spectrum above 450 keV. The TAC time spectrum after background is shown in Fig. 9. The prompt peak in this spectrum is a result of prompt coincidences between the 433.7-keV γ ray and other transitions in ^{142}Pm. Using the computer code KINFIT,[15] we obtained a half-life of 0.63 ± 0.02 μsec for the 628.6-keV state. The delayed γ-γ spectrum, gated on the 0.2—1.8-μsec region of the TAC spectrum, is shown in Fig. 10, and the delayed γ-γ results are given in Table V.

837.1-keV state

This state was observed in the (p,2nγ) reaction, but there the 640.5-keV γ ray to the 196.6-keV state was observed, while in the $(\alpha,4n\gamma)$ reaction we observed instead a 108.9-keV γ ray to the 728.3-keV state. (The 837.1- and 208.7-keV γ rays were observed in both reactions.) The $(\alpha,4n\gamma)$ angular distributions are consistent with the (p,2nγ) assignment of $\frac{9}{2}^+$.

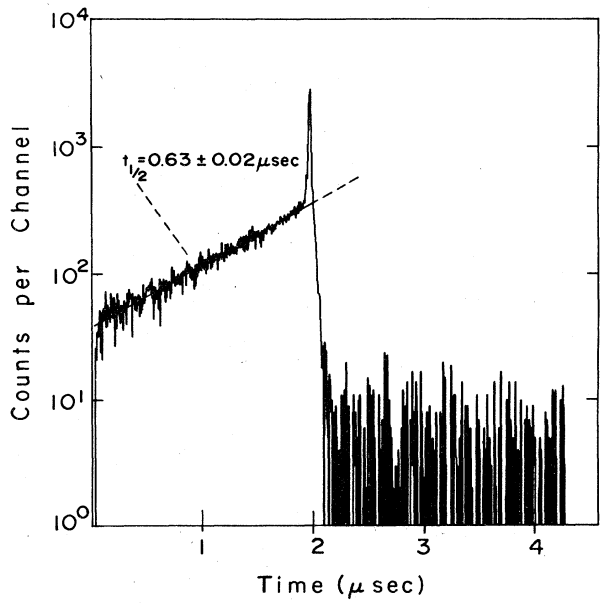

FIG. 9. Time-to-amplitude conversion spectrum used to determine the half-life of the 628.4-keV state in ^{141}Pm.

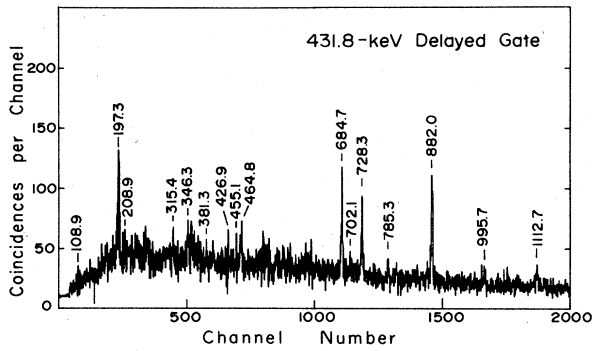

FIG. 10. ^{141}Pm delayed coincidence spectrum. This spectrum enhances the transitions that feed (directly or indirectly) into the 628.4-keV, 0.63-μsec state.

Other states seen in both the (α,4nγ) and (p,2nγ) reactions

The ten states at 974.2, 1108.0, 1313.3, 1359.6, 1510.6, 1628.1, 1969.9, 2015.4, 2098.8, and 2238.9 keV were seen in both reactions. Generally, placements of these states are based on γ-γ coincidence data, delayed γ-γ coincidence data, intensity balances, and summing relationships supported by both reactions. The J^π assignments (and limitations) were made on the basis of angular distribution coefficients and, where known, transition multipolarities. Where there were large errors on the A_2 or A_4 values from one reaction, the set from the other reaction was chosen. [This is why the assignments for the 1628.1-, 2015.4-, and 2238.9-keV states, for example, were made using the (α,4nγ) reaction data.] The 1414.5-keV state seen in the (p,2nγ) reaction was probably also seen in the (α,4nγ) reaction, but here we did not observed its 247.4-keV γ ray, leaving only a member of the 785.3-keV doublet to prove its population by this reaction.

TABLE V. ^{141}Pr(α,4nγ)^{141}Pm results for 431.8-keV delayed gate.

E_γ (keV)	I_γ[a]
108.9	9.4
197.3	41
208.9	7.6
315.4	11.3
346.3	10.4
381.3	8.0
426.9	6.7
455.1	0.9
464.8	15.4
684.7	60
702.1	21
728.3	61
785.3	26
882.0	$\equiv$100
995.7	11.8
1112.7	24

[a]The errors on the intensities are $\approx \pm 10\%$.

1055.3-keV state

The coincidence relationship between the 426.9- and 455.1-keV γ rays, the delayed coincidence between the 426.9- and 431.8-keV γ rays, the intensity balance, and the energy sums lead us to place a new state [not seen previously via either β decay or the (p,2nγ) reaction] at 1055.3 keV.

The angular distribution coefficients for the 426.9- and 455.1-keV γ rays restrict the J^π of this state to $\frac{11}{2}^-$ or $\frac{13}{2}^-$. The fact that this state is not fed by γ rays from high-spin states lying above it indicates that most likely it is not in the yrast sequence, eliminating the $\frac{13}{2}^-$ possibility (as discussed in connection with the 1313.3-keV state in Sec. III A). Thus, we assign it $\frac{11}{2}^-$.

High-lying high-spin states

The four states at 1891.9, 2554.3, 2703.7, and 3004.6 keV are high-lying, high-spin states populated only via the (α,4nγ) reaction—all clearly established by coincidence relationships. The possible J^π assignments for these states are based on the A_2 and A_4 values of their deexciting γ rays. Except for the $\frac{17}{2}^-$ 1891.9-keV state, no unique assignments were possible.

The metastable state at 2530.9 keV

The 639.0- and 1020.3-keV γ rays deexciting the 2530.9-keV state are isotropic, and the γ-γ coincidence experiments showed no γ rays feeding the 2530.9-keV state. Perhaps it is a metastable state. A precise determination of its half-life was not possible from our current data, but there is a clear indication that its half-life is greater than about 2 μsec.

The 639.0-keV transition to the $\frac{17}{2}^-$ 1891.9-keV state is the rate-determining one (90% of the deexcitation goes through it), so it can be used to determine the J^π of the 2530.9-keV state. Single-particle estimates[16] of the half-lives are as follows: $E2$ (1.2×10^{-10} sec), $M2$ (2.9×10^{-9} sec), $E3$ (2.3×10^{-5} sec), $M3$ (2.5×10^{-4} sec), $E4$ (6.6 sec), and $M4$ (4.1 sec). Thus, it is probably an $E3$, implying $J^\pi=\frac{23}{2}^+$ for the 2530.9-keV state. Such an assignment would lead to the 1020.3-keV transition being an $M4$, with a single-particle prediction of 0.61 sec for its half-life. The 1020.3-keV is much too intense for this prediction. (Assignments of $M3$ and $E4$ for the 639.0- and 1020.3-keV transitions predict only slightly better agreement for the branching ratio.)

Metastable states occur in nearby odd-odd nuclides:[17] a 2.0-msec 8^- state at 883.2 keV in ^{142}Pm and a 1.0-μsec 8^- state at 1128.4 keV in ^{144}Eu, which were assigned to the configuration $\pi d_{5/2}\times\nu h_{11/2}$. One cannot put too much faith in γ-ray transition probabilities—both of these states decay by transitions only slightly retarded (by a factor of 6.5 for the $E3$ in ^{142}Pm and 40 for the $E2$ in ^{144}Eu) over the single-particle estimates; yet, both are simplistically double-particle transitions. The even-parity states, in particular, in these nuclei are not at all pure, which leads to small components of the wave functions being responsible for most of the γ-ray transition probabilities.

At the energy of 2530.9 keV in ^{141}Pm a three-quasiparticle state could easily explain this metastable state. Assuming $\frac{25}{2}^+$, one could produce this by coupling either $\pi d_{5/2}$ or $\pi g_{7/2}^{-1}$ to $(\nu h_{11/2})^2_{10+}$. On the other hand, a $\frac{25}{2}^-$ assignment could be explained as the highest spin member of $\pi d_{5/2} \times \pi g_{7/2}^{-1} \times \nu h_{11/2}$. Various collective (e.g., triaxial) configurations could also enter. Clearly, more information is needed to determine the exact configuration of this state.

C. Comparisons between the (p,2nγ) and (α,4nγ) reactions and with other experimental results

A summary of the present knowledge of levels in $^{141}_{61}Pm_{80}$ is shown in Fig. 11. States in the first two columns are based on our present in-beam results, and these are compared in the third column with results from $^{141}Sm^{m+g}$ decays. The state at 1055.3 keV seen via the $(\alpha,4n\gamma)$ reaction is not necessarily the same state as that seen via $^{141}Sm^m$ decay at 1046.4 keV. From this figure it can be seen that, as expected, the $(\alpha,4n\gamma)$ reaction did populate many higher-spin states not seen in β decay or the (p,2nγ) reaction. Our data are more extensive than those of Piiparinen *et al.*,[4] and most of the comparisons were made during the discussions of the individual levels. We agree on all but five levels below 2 MeV but disagree on a number of higher-lying levels.

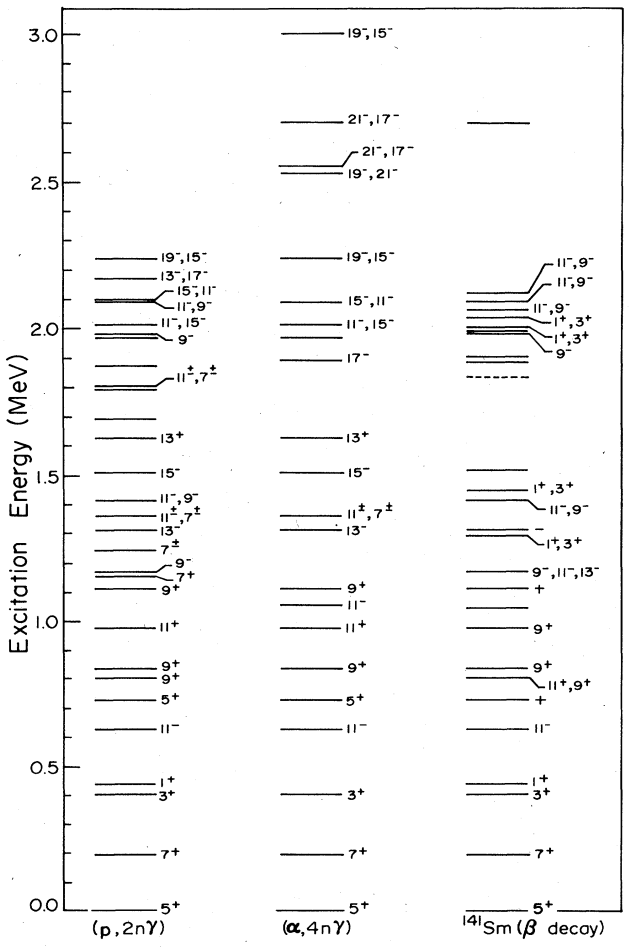

FIG. 11. Summary of known energy levels in $^{141}_{60}Pm_{80}$. Spins are shown as $2J$. The levels in the first two columns are from the present work; those in the third column, from Refs. 5 and 6.

V. DISCUSSION

A. Single-quasiparticle states

The five lowest-lying states in ^{141}Pm, all seen via the (p,2nγ) reaction as well as from β decay, are presumed to be best described as the five single-quasiparticle shell-model states lying between $Z=50$ and 82. They lie at 0 ($\pi d_{5/2}$), 196.6 ($\pi g_{7/2}^{-1}$), 403.8 ($\pi d_{3/2}$), 438.8 ($\pi s_{1/2}$), and 628.4 keV ($\pi h_{11/2}$). The $s_{1/2}$ state was not populated appreciably either directly or indirectly by the $(\alpha,4n\gamma)$ reaction, as anticipated.

Relatively little has been done in the way of shell-model calculations in this region, primarily because of the cumbersomeness of including fractional-parentage coefficients for the $h_{11/2}$ state in the present computer codes. However, for $N=80$ in general these five states have been analyzed by de Takacsy and Das Gupta[18] as single-quasiparticle states. And extrapolations of the older pairing-plus-quadrupole calculations of Kisslinger and Sorensen[19] give remarkable agreement.

One important difference between ^{141}Pm and ^{143}Eu (cf. Ref. 1) should be mentioned here: The $\pi d_{3/2}$ state does not appear to be so fractionated in ^{141}Pm as it is in ^{143}Eu; i.e., the 403.8-keV state in ^{141}Pm appears to contain the major fraction of the $\pi d_{3/2}$ strength. In ^{143}Eu the lowest $\frac{3}{2}^+$ state, at 258.81 keV, had primarily a $[\pi d_{5/2} \times 2^+]_{3/2+}$ configuration, with much of the $\pi d_{3/2}$ strength occurring in a state at 819.9 keV.

B. Negative-parity collective states

The negative-parity states in ^{141}Pm can be described from two contrasting viewpoints: One is the three-quasiparticle approach that was used to describe those high-lying states selectively populated by $^{141}Sm^m$ β^+/ϵ decay.[2] The other is the triaxial weak-coupling model,[5] which we use here to describe the other negative-parity states. In many ways these two approaches are but extremes of the same basic, physically oriented picture. It is hoped that the more abstract, group-theoretical approach of the interacting boson-fermion model[20,21] can be extended to this region of nuclei below $N=82$ in the near future.

The ^{141}Pm negative-parity states are expected to consist primarily of the $\pi h_{11/2}$ state coupled to a $^{140}_{60}Nd_{80}$ (triaxial) core. There is evidence that the 2^+ one-phonon quadrupole vibrational state lies[22] at $\approx$770 keV in ^{140}Nd. The ^{141}Pm 1167.1-keV $\frac{9}{2}^-$ state is presumably a coupling of the $\pi h_{11/2}$ state to this core state, lying as it does at the expected energy. It is expected to contain significant admixtures, however, especially of three-quasiparticle states. Systematically, it corresponds to the 977.47-keV state in ^{143}Eu.

The 1414.5-keV state feeds into the 1167.1-keV state, implying a $[\pi h_{11/2} \times 2_1^+]_{11/2-}$ assignment. The primary

component of the 1313.3-keV state is thus assumed to be $[\pi h_{11/2} \times 2_1^+]_{13/2^-}$. The 1510.6-keV state also deexcites through the $\frac{11}{2}^-$ 1167.1-keV state, so we tentatively identify it with the $[\pi h_{11/2} \times 2_1^+]_{15/2^-}$ component.

These preliminary considerations aside, we performed a complete triaxial-coupling calculation, similar to the one performed for states in ^{143}Eu,[1] coupling the available single-particle states to the 2_1^+, 0_2^+, 2_2^+, 4_2^+, and 3_1^- vibrational states in ^{140}Nd. Our results for the negative-parity states are shown in Fig. 12, where they are compared with the experimental states. The calculation was performed for both prolate and oblate shapes, and it can be seen that the agreement is somewhat better for an oblate shape. This was also found to be true for ^{143}Eu, with the prolate calculation predicting the wrong order for many of the states; predicting, for example, a low-lying $\frac{7}{2}^-$ state that is not seen. The agreement between calculation and experiment is actually better for ^{141}Pm than it was for ^{143}Eu, and, although this may be partly fortuitous, there is some indication that the positive-parity single-quasiparticle states are purer (not so fractionated) in ^{141}Sm than in ^{143}Eu (cf. Sec. V A above), making this simple model more applicable. Whether or not this holds true for the negative-parity single-quasiparticle states remains to be seen, but these rather simple calculations point in that direction.

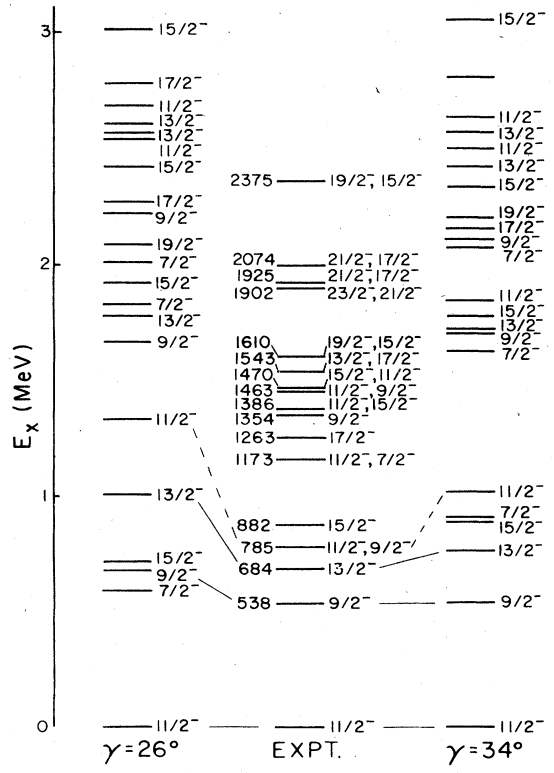

FIG. 12. Energies of negative-parity triaxial core-coupled ^{141}Pm states compared with our experimental results. These were calculated for coupling the $\pi h_{11/2}$ state to a deformed ^{140}Nd core, the states on the left for a prolate deformation, on the right for an oblate deformation. An oblate deformation seems to be indicated. (All energies are given relative to the single-particle $\pi h_{11/2}$ state.)

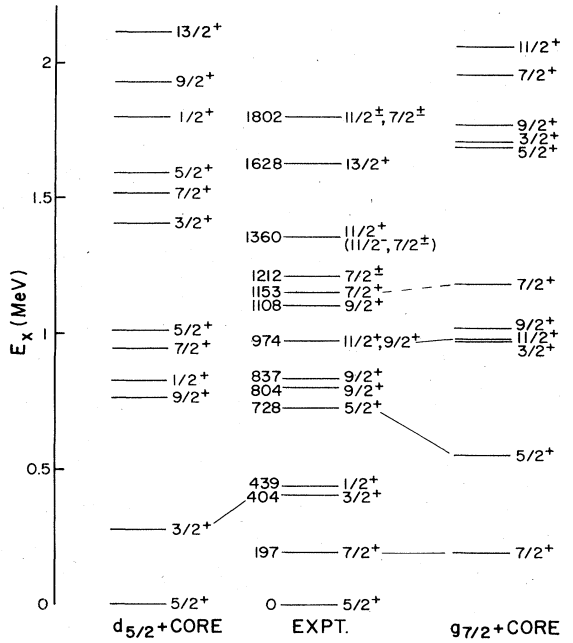

FIG. 13. Energies of positive-parity triaxial core-coupled ^{141}Pm states compared with our experimental results. Only $\pi d_{5/2}$ and $\pi g_{7/2}^{-1}$ states coupled to an oblate core ($\gamma = 34°$) are shown.

C. Positive-parity collective states

In Fig. 13 we show results from the calculations for coupling the $\pi d_{5/2}$ and $\pi g_{7/2}^{-1}$ states to the same triaxial core. An oblate core was assumed for both. Because of the large number of positive-parity states available, one would expect far more configuration mixing and consequently poorer agreement with experiment than for the negative-parity states. To some extent this is true; yet the agreement is not really bad, especially for the $\pi g_{7/2}^{-1}$ state plus core. However, closer inspection reveals that much of the agreement could be fortuitous, and results from such simple calculations should be treated with caution.

The $\pi d_{3/2}$ state at 403.8 keV, for example, appears to be less fractionated in ^{141}Pm than in ^{143}Eu; yet, our calculations would have us believe that the lowest $\frac{3}{2}^+$ state is a $\pi d_{5/2}$ core-coupled state. Also, consider the two $\frac{9}{2}^+$ states at 804.5 and 837.1 keV. Their major γ-ray deexcitation patterns point toward the 804.5-keV state containing mostly the $\pi g_{7/2}^{-1}$-coupled configuration and the 837.1-keV state containing mostly the $\pi d_{5/2}$-coupled configuration. Within reason the calculations support this, producing two states at the appropriate locations. However, the deexcitation of the 837.1-keV state, in particular, shows that not only is this state highly mixed, but also it must contain some sort of $\pi h_{11/2}$ component (perhaps $\pi h_{11/2}$ coupled to an octupole core, not included in our calculations). Our present calculations certainly support the idea of an oblate deformation, but it is difficult to make a one-to-one correlation between the calculated and

experimental states. More extensive calculations, including configuration mixing, need to be performed before quantitative conclusions can be drawn.

This material is based upon work supported by the U.S. National Science Foundation under Grants No. PHY 76-04912 and PHY 78-01684.

---

*Present address: Department of Physics, University of Manitoba, Winnipeg, Manitoba, Canada R3T 2N2.

†Present address: Daresbury Laboratory, Daresbury, Warrington WA4 4AD, England.

‡Present address: Nuclear Science Division, Lawrence Berkeley Laboratory, Berkeley, California 94720.

[1]R. Aryaeinejad, R. B. Firestone, W. H. Bentley, and Wm. C. McHarris, Phys. Rev. C **23**, 194 (1981).

[2]R. E. Eppley, R. R. Todd, Wm. C. McHarris, and W. H. Kelly, Phys. Rev. C **5**, 1084 (1972).

[3]G. G. Kennedy, J. Deslauriers, S. C. Gujrathi, and S. K. Mark, Phys. Rev. C **15**, 792 (1977).

[4]M. Piiparinen, M. Kortelahti, A. Pakkhanen, T. Kompa, and R. Komn, Nucl. Phys. **A342**, 53 (1980).

[5]J. Meyer-ter-Vehn, Nucl. Phys. **A249**, 111 (1975).

[6]CS8N, computer code written by T. Sikkeland and D. Lebeck, Lawrence Berkeley Laboratory; adapted for NSCL Sigma-7 computer by C. Morgan (1975).

[7]S. Raman, J. L. Forster, O. Dietzsch, D. Spaulding, L. Bimbot, and B. H. Wildenthal, Nucl. Phys. **A201**, 21 (1973).

[8]J. T. Routti and S. G. Prussin, Nucl. Instrum. Methods **72**, 125 (1969).

[9]GADFIT, computer code written by R. A. Warner, NSCL (1976).

[10]F. Y. Yap, R. R. Todd, W. H. Kelly, Wm. C. McHarris, and R. A. Warner, Phys. Rev. C **11**, 952 (1975).

[11]C. Eckström, S. Ingleman, M. Olsmats, and B. Wannberg, Phys. Scr. **6**, 181 (1972).

[12]R. A. Warner, R. R. Todd, R. E. Eppley, W. H. Kelly, and Wm. C. McHarris, Bull. Am. Phys. Soc. **16**, 1161 (1971).

[13]R. Arl't, G. Beyer, Y. Vavryschuk, V. A. Morosov, T. M. Muminov, V. I. Rasov, J. Sazynski, H. Fuia, H. Strusny, and E. Herrmann, Joint Institute for Nuclear Research (USSR) Report No. P6-5517, 1970 (unpublished).

[14]E. Newman, K. S. Toth, R. L. Auble, R. M. Gaedke, M. F. Roche, and B. H. Wildenthal, Phys. Rev. C **1**, 1118 (1970).

[15]J. L. Dye and V. A. Nicely, J. Chem. Educ. **48**, 443 (1971).

[16]S. A. Moszkowski, in *Alpha, Beta and Gamma-Ray Spectroscopy*, edited by K. Siegbahn (North-Holland, Amsterdam, 1965), Chap. XV.

[17]L. Funke, W. D. Fromm, H. J. Keller, R. Arl't, and P. M. Gopytsch, Nucl. Phys. **A274**, 61 (1976).

[18]N. de Takacsy and S. Das Gupta, Phys. Rev. C **13**, 399 (1976).

[19]L. S. Kisslinger and R. A. Sorensen, K. Dan. Vidensk. Selsk. Mat.-Fys. Medd. **32**, No. 9 (1960).

[20]F. Iachello and O. Scholten, Phys. Rev. Lett. **43**, 679 (1979).

[21]O. Scholten and N. Blaei, Nucl. Phys. **A380**, 509 (1982).

[22]V. V. Renaev, Yu. S. Korda, and A. P. Klyucharen, Izv. Akad. Nauk SSSR, Ser. Fiz. **27**, 125 (1963).